# 1,3-Ditungstacyclobutadienes. 2.[1] The Synthesis of Alkoxide Derivatives of $W_2(\mu\text{-}CSiMe_3)_2(CH_2SiMe_3)_4$ and Investigations of the Electronic Structures of the $M_2(\mu\text{-}CSiMe_3)_2$ Core as a Function of $d^n$–$d^n$ Interactions ($n$ = 0, M = Ta; $n$ = 1, M = W; $n$ = 2, M = Re)

Malcolm H. Chisholm,*[2a] Joseph A. Heppert,[2a] Edward M. Kober,[2b] and Dennis L. Lichtenberger*[2b]

*Department of Chemistry, Indiana University, Bloomington, Indiana 47405, and the Laboratory for Electron Spectroscopy and Surface Analysis, Department of Chemistry, University of Arizona, Tucson, Arizona 85721*

*Received August 19, 1986*

$W_2(\mu\text{-}CSiMe_3)_2(CH_2SiMe_3)_4$ (I) reacts with *t*-BuOH in alkane solvents to produce a mixture of two isomers of $W_2(\mu\text{-}CSiMe)_2(O\text{-}t\text{-}Bu)_2(CH_2SiMe_3)_2$ from which the minor isomer can be isolated by fractional crystallization. The electronic structures of several related dimetallacyclobutadiene derivatives have been investigated by UV photoelectron spectroscopy, UV/visible spectrophotometry, and MO calculations. The M–M bonding configurations for the $M_2(\mu\text{-}CSiMe_3)_2(CH_2SiMe_3)_4$ molecules have been determined as $\sigma^0\delta^{*0}$, $\sigma^2\delta^{*0}$, and $\sigma^2\delta^{*2}$ for M = Ta, W, and Re, respectively, by EHMO and Fenske–Hall MO calculations. This result is better reconciled with the previously observed M–M distances—$Nb_2 > Re_2 > W_2$—than with the original proposal of a $\sigma^2\pi^2$ configuration for the Re derivative. On replacement of the terminal alkyl ligands of the W complex by O-*i*-Pr ligands, the $2a_u$ LUMO (W–W $\delta^*$) and $2b_{2g}$ W–$\mu$-C $\pi$ bond are strongly destabilized by antibonding interactions with p$\pi$ orbitals on oxygen. Destabilization of the $2b_{2g}$ orbital results in the appearance of a clearly defined ionization representing this orbital at 7.2 eV in the PE spectrum of $W_2(\mu\text{-}CSiMe_3)_2(O\text{-}i\text{-}Pr)_4$. Mulliken population analyses of the $6a_g$ orbitals of I and $W_2(\mu\text{-}CSiMe_3)_2(O\text{-}i\text{-}Pr)_4$ correctly predict that I prefers a shorter W–W distance of 2.54 Å, while the alkoxide-substituted compound prefers the longer W–W distance of 2.62 Å.

## Introduction

Our interest in the chemistry of unsaturated dimetallacycles was sparked by the variety of products obtained from the reactions of $W_2(O\text{-}t\text{-}Bu)_6$ with alkynes. Schrock and co-workers[3-5] demonstrated that terminal alkylidyne complexes were formed during the reactions involving MeCCMe, EtCCEt, and a variety of functional group substituted acetylenes. Furthermore, they showed that the metathesis-like reaction between the M–M and C–C triple bonds was not limited to O-*t*-Bu ligands but was also operative for O-*i*-Pr and $OC(CF_3)Me_2$ ligands. Meanwhile in our laboratories we have found evidence for the existence of an equilibrium between alkylidyne complexes $(RO)_3W{\equiv}CR'$ and perpendicular alkyne adducts of formula $W_2(OR)_6(\mu\text{-}C_2R'_2)(py)_n$, where $n$ = 1 or 2. This was first discovered for R = *t*-Bu and R′ = H[6] and subsequently extended to include R = *i*-Pr and R′ = Me and R = *t*-$BuCH_2$ and R′ = Me, Et, and Ph.[7]

Although there has been some speculation concerning the reaction pathway leading to C–C bond cleavage from a dimetallatetrahedrane and its reverse,[4,8] no intermediates have been isolated. The two most plausible intermediates involve 1,2- or 1,3-dimetallacyclobutadienes. This prompted us to turn our attention to the chemistry of $(Me_3SiCH_2)_4W_2(\mu\text{-}CSiMe_3)_2$ (I), which has a planar 1,3-$M_2C_2$ core. Although our studies to date have not uncovered any evidence for the conversion of a planar 1,3-$W_2(\mu\text{-}CSiMe_3)_2$ core into either two $W{\equiv}CSiMe_3$ moieties or the dimetallatetrahedrane $W_2(\mu\text{-}C_2(Si_2Me_3)_2)$ core, we have probed the reactivity of the 1,3-$M_2(\mu\text{-}CSiMe_3)_2X_4$ compounds both as a function of metal and $d^n$ configuration (M = Ta, $d^0$–$d^0$; M = W, $d^1$–$d^1$) and the nature of the terminal ligands (X = $Me_3SiCH_2$ and *i*-PrO).

Compound I (M = W) has been shown to undergo three types of reactions. (1) In hydrocarbon solvents, the addition of alcohols leads to the replacement of $Me_3SiCH_2$ ligands by OR ligands and even one of the $\mu$-$CSiMe_3$ ligands as exemplified by the reactions shown in eq 1[1] and 2.[9]

$$(Me_3SiCH_2)_4W_2(\mu\text{-}CSiMe_3)_2 + i\text{-}PrOH(\text{excess}) \xrightarrow[\text{hexane}]{25\ ^\circ C} (i\text{-}PrO)_4W_2(\mu\text{-}CSiMe_3)_2 + 4Me_4Si \quad (1)$$

$$(Me_3SiCH_2)_4W_2(\mu\text{-}CSiMe_3)_2 + EtOH(\text{excess}) \xrightarrow[\text{hexane}]{25\ ^\circ C} {}^1/_2W_4(\mu\text{-}CSiMe_3)_2(OEt)_{14} + 5Me_4Si \quad (2)$$

(2) Halogens (X = Cl, Br, and I) and diisopropyl peroxide effect a homolytic oxidative cleavage of the W–W bond in I, yielding a new class of 1,3-ditungstacyclobutadienes of formula $[X(Me_3SiCH_2)_2W(\mu\text{-}CSiMe_3)]_2$ (II).[10]

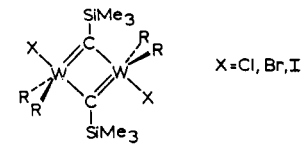


(1) Part 1. Chisholm, M. H.; Heppert, J. A.; Huffman, J. C. *J. Am. Chem. Soc.* **1985**, *107*, 5116.
(2) (a) Indiana University. (b) Arizona University.
(3) Schrock, R. R.; Listemann, M. L.; Sturgeoff, L. G. *J. Am. Chem. Soc.* **1982**, *104*, 4291.
(4) Listemann, M. L.; Schrock, R. R. *Organometallics* **1985**, *4*, 74.
(5) Freudenberger, J. H.; Pedersen, S. F.; Schrock, R. R. *Bull. Soc. Chim. Fr.* **1985**, 349.
(6) Chisholm, M. H.; Folting, K.; Hoffman, D. M.; Huffman, J. C. *J. Am. Chem. Soc.* **1984**, *106*, 6794.
(7) Chisholm, M. H.; Conroy, B. K.; Hoffman, D. M.; Huffman, J. C., results to be published.
(8) Chisholm, M. H.; Hoffman, D. M.; Huffman, J. C. *Chem. Soc. Rev.* **1985**, *14*, 69.
(9) Chisholm, M. H.; Heppert, J. A.; Hoffman, D. M.; Huffman, J. C. *J. Am. Chem. Soc.* **1984**, *107*, 1234.
(10) Chisholm, M. H.; Heppert, J. A.; Huffman, J. C.; Thornton, P. *J. Chem. Soc., Chem. Commun.* **1985**, 1466.

0276-7333/87/2306-1065$01.50/0 

The molecular structures of the compounds where X = Cl and Br have been determined by single-crystal X-ray crystallography and found to adopt a common geometry based on the fusing of two trigonal-bipyramidal environments as shown diagramatically (W–W = 2.75 Å).[10]

The compounds II are unusual in displaying temperature-dependent paramagnetism both in solution and in the solid state, despite the fact that the tungsten atoms are formally in the +6 oxidation state making II formally $d^0$–$d^0$ complexes.

(3) A wide variety of $\pi$-acceptor ligands promote heterolytic oxidative cleavage of the W–W bond in I to yield 1:1 adducts that may be described by the valence bond description shown in III.

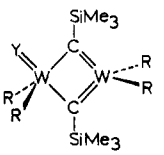


Similar adduct formation is not seen in the chemistry of the $d^0$–$d^0$ tantalum compound, emphasizing the importance of metal $d\pi$ back-bonding in the stabilization of III.

During the course of these studies, we have observed that the relative stability of the 1:1 adducts III followed the order $Ph_2CN_2$[11] $\gg$ R′C≡CR′[1] > RCH=C=CHR′[12] > RNC $\approx$ CO,[13] which correlates roughly with the anticipated Y–W multiple-bond strength. A stabilization of the Y–W multiple bond, however, has a retarding influence on the rate of attack by Y on the bridging alkylidyne ligand, and this in turn can be influenced by the supporting ligands OR vs. $CH_2SiMe_3$. For example, alkoxides that are good $\pi$ donors[15] have a destabilizing influence on 1:1 adduct formation in reactions with alkynes and allenes but promote C–C bond forming with the alkylidyne ligand.[1,16]

In an effort to understand some of the factors affecting the structural parameters and reactivity patterns of the $M_2(\mu\text{-}CSiMe_3)_2$ core, we decided to undertake a study of the electronic structure of the parent complexes $M_2(\mu\text{-}CSiMe_3)_2X_4$, where M = Ta,[17] W,[18,19] or Re[20] with X = $CH_2SiMe_3$ and M = W with X = OR.[1] We describe here the results of molecular orbital calculations employing the method of Fenske and Hall[21] along with photoelectron spectra for some of the complexes. Further studies of the reaction of I with alcohols are also described.

## Results and Discussion

**Synthesis of Alkoxy- and Phenoxy-Substituted Compounds. General Features.** The replacement of $CH_2SiMe_3$ by OR or OAr ligands appears to be largely determined by steric considerations. For reactions employing $W_2(\mu\text{-}CSiMe_3)_2(CH_2SiMe_3)_4$ we have previously reported on the reactions with EtOH and *i*-PrOH that proceed according to eq 2 and 1, respectively. The reaction with *t*-BuOH in benzene proceeds more slowly, and at room temperature substitution of only two $Me_3SiCH_2$ ligands is apparently favored. The compound so formed, $(t\text{-BuO})_2(Me_3SiCH_2)_2W_2(\mu\text{-}CSiMe_3)_2$, appears to be a mixture of two isomers as shown by the $^1H$ NMR spectrum in Figure 1. Tentatively, we assign this to a mixture of syn and anti isomers that arise from the substitution at each tungsten atom of one $Me_3SiCH_2$ ligand by one O-*t*-Bu. From the $^1H$ NMR spectrum, we cannot rule out the possibility that one of the isomers is a gem-disubstituted species, $(t\text{-BuO})_2W(\mu\text{-}CSiMe_3)_2W(CH_2SiMe_3)_2$. By fractional crystallization we have been able to separate the two isomers, though some residual impurity of the other isomer is always present upon the first crystallization process. Regretably, single-crystal X-ray studies have not been possible because crystals were either twinned or unsuitable for detailed work. The point that is to be recognized is that at least one of the isomers is either the syn or the anti isomer. This point will become of considerable significance when we examine the stereochemistry of certain reactions since the isomers formed in the reaction between I and *t*-BuOH do not interconvert to any significant extent at room temperature in benzene over a period of several days.

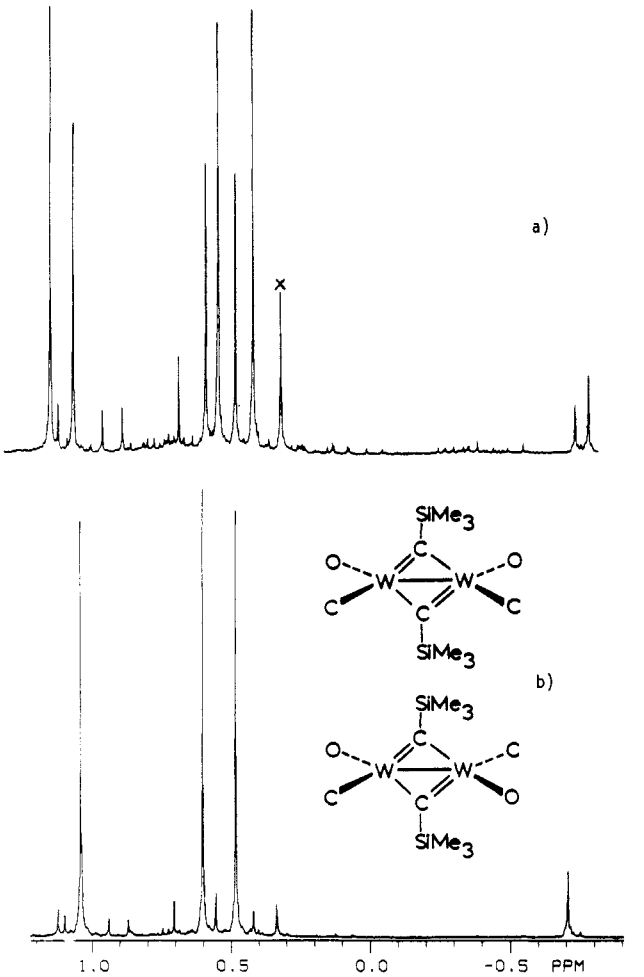


**Figure 1.** 360-MHz $^1H$ NMR spectra of the syn and anti isomers of $W_2(\mu\text{-}CSiMe_3)_2(CH_2SiMe_3)_2(O\text{-}t\text{-}Bu)_2$ showing (a) the crude reaction mixture and (b) the purified minor isomer.

Reactions between I and phenol and mesityl alcohols gave a mixture of what appeared to be partially $Me_3SiCH_2$-substituted products, but no single crystalline compound was separated. Compound I displayed no ev-

(11) Chisholm, M. H.; Heppert, J. A.; Huffman, J. C., results to be published.
(12) Chisholm, M. H.; Folting, K.; Heppert, J. A.; Streib, W. E. *J. Chem. Soc., Chem. Commun.* **1985**, 1755.
(13) Chisholm, M. H.; Heppert, J. A.; Huffman, J. C.; Streib, W. A. *J. Chem. Soc., Chem. Commun.* **1985**, 1771.
(14) Alkynes, but not RNC and CO ligands, can act as $\pi$ donors as well as $\pi$ acceptors.
(15) Chisholm, M. H. *Polyhedron* **1983**, *2*, 681.
(16) Chisholm, M. H.; Heppert, J. A. *Adv. Organomet. Chem.* **1986**, *27*, 97.
(17) Huq, F.; Mowat, W.; Skapski, A. C.; Wilkinson, G. *J. Chem. Soc., Chem. Commun.* **1971**, 1477.
(18) Andersen, R. A.; Gayler, A. L.; Wilkinson, G. *Angew. Chem., Int. Ed. Engl.* **1976**, *15*, 609.
(19) Chisholm, M. H.; Cotton, F. A.; Extine, M. W.; Murillo, C. A. *Inorg. Chem.* **1978**, *17*, 696.
(20) Bochmann, M.; Wilkinson, G.; Galas, A. M. R.; Hursthouse, M. B.; Abdul-Malik, K. M. *J. Chem. Soc., Dalton Trans.* **1980**, 1797.
(21) Hall, M. B.; Fenske, R. F. *Inorg. Chem.* **1972**, *11*, 768.

**Table I. Pertinent Structural Parameters for the 1,3-Dimetallacyclobutadienes**

| compd | M–M, Å | M–$\mu$-C, Å | M–C–M, deg | X–M–X, deg | ref |
|---|---|---|---|---|---|
| $Nb_2(\mu\text{-}CSiMe_3)_2(CH_2SiMe_3)_4$ | 2.897 (2) | 1.98 (av) | 94.4 (4) | not given | 17 |
| $W_2(\mu\text{-}CSiMe_3)_2(CH_2SiMe_3)_4$ | 2.535 (av) | 1.89 (av) | 84 (av) | 114 (av) | 19 |
| $W_2(\mu\text{-}CSiMe_3)_2(O\text{-}i\text{-}Pr)_4$ | 2.620 (av) | 1.92 (av) | 85.6 (av) | 114.8 (7) | 1 |
| $W_2(\mu\text{-}CPh)_2(O\text{-}t\text{-}Bu)_4$ | 2.665 (1) | 1.94 (1) | 86.9 (4) | 114.1 (4) | 23 |
| $Re_2(\mu\text{-}CSiMe_3)_2(CH_2SiMe_3)_4$ | 2.557 (1) | 1.929 (9) | 83.0 (3) | 114.8 (4) | 20 |

idence of reaction with 4 equiv of 2,4,6-tri-*tert*-butylphenol (2,4,6-TBP) in toluene after 8 h at 60 °C. However, Rothwell[22] has found that 2,4,6-TBP in excess does react with I at 80 °C over several weeks to give substitution of one $Me_3SiCH_2$ ligand: $(2,4,6\text{-}t\text{-}Bu_3C_6H_2O)(Me_3SiCH_2)_3W_2(\mu\text{-}CSiMe_3)_2$.

The tantalum analogue of I appears more reactive toward alcohols and substituted phenols. The reaction between $(Me_3SiCH_2)_4Ta_2(\mu\text{-}CSiMe_3)_2$ and *i*-PrOH proceeds to give $Ta(O\text{-}i\text{-}Pr)_5$ with elimination of $Me_4Si$, and we have not been able to isolate a pure compound of formula $(RO)_4Ta_2(\mu\text{-}CSiMe_3)_2$. However, Rothwell[22] has found that reactions employing an excess of 2,4,6-tri-*tert*-butylphenol proceed to give $(Me_3SiCH_2)_2(2,4,6\text{-}Bu_3C_6H_2O)_2Ta_2(\mu\text{-}CSiMe_3)_2$ and a single-crystal X-ray determination has established the gem OAr substitution pattern.

It is evident that the tantalum–carbon bonds are more susceptible to protolysis in reactions involving alcohols and phenols relative to the tungsten–carbon bonds in the related $(Me_3SiCH_2)_4M_2(\mu\text{-}CSiMe_3)_2$ compounds. The Ta–C bonds are, however, unreactive toward C–C bond formation in their reactions with alkynes, allenes, RNC, and CO whereas the $W_2(\mu\text{-}CSiMe_3)_2$ moiety is reactive to each of the above.[16] The currently reported[20] route to $(Me_3SiCH_2)_4Re_2(\mu\text{-}CSiMe_3)_2$ does not make analogous studies feasible.

**Structural Parameters for $X_4M_2(\mu\text{-}CR)_2$ Compounds.** Structural parameters for the 1,3-dimetallacyclobutadienes are summarized in Table I. The ditantalum compound is known to be isostructural with the diniobium compound and would most surely display similar distances and angles.[17] Included in Table I are data for the compound $(t\text{-}BuO)_4W_2(\mu\text{-}CPh)_2$ that was isolated by Cotton and co-workers[23] as one of the products formed in the reaction between $W_2(O\text{-}t\text{-}Bu)_6$ and PhC≡CPh in hexane at ca. 60 °C. It is seen to be essentially identical with $(i\text{-}PrO)_4W_2(\mu\text{-}CSiMe_3)_2$ in terms of the central $O_4W_2(\mu\text{-}C)_2$ core. The following points are worthy of note.

(1) For compounds of formula $(Me_3SiCH_2)_4M_2(\mu\text{-}CSiMe_3)_2$ there is a notable contraction in the M–M distance in going from M = Nb ($d^0$–$d^0$) to M = W ($d^1$–$d^1$) and the distance 2.535 Å (averaged) is typical of a W–W single-bond distance for W(V)–W(V) containing compounds supported by bridging oxo ligands.[24] The distance in the $d^2$–$d^2$ dinuclear compound for M = Re is, however, slightly longer than the W–W distance. This is not consistent with the original suggestion[20] for the existence of a Re–Re double bond, $\sigma^2\pi^2$.

(2) Substitution of RO for $Me_3SiCH_2$ causes a significant lengthening of the W–W bond distance, ca. 0.1 Å. The W–$\mu$-C distances are also significantly lengthened by OR for $Me_3SiCH_2$ substitution.

(3) Changes in the central M–C–M angle can be understood in terms of the change in M–M distance.

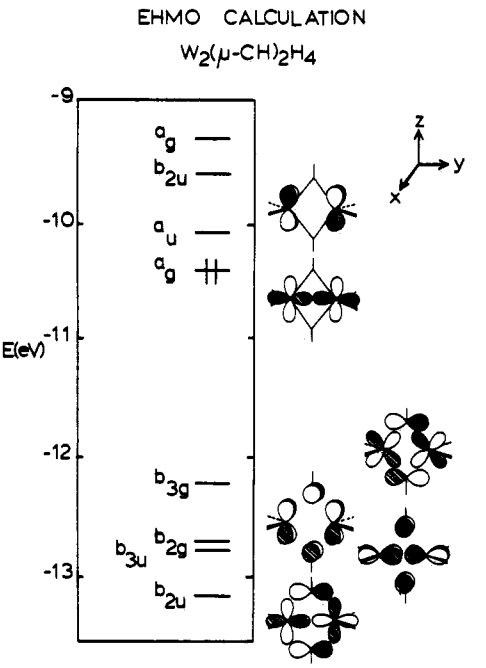


**Figure 2.** Results of the EHMO calculation on $W_2(\mu\text{-}CH)_2H_4$.

(4) The external angles X–M–X where X = O or C and M = Nb, W, and Re are essentially invariant to the $d^n$–$d^n$ interaction ($n$ = 0, 1, and 2) and the external substituents, $Me_3SiCH_2$ vs. RO.

The questions of fundamental interest that arise within this series are (1) do the Ta, W, and Re analogues have M–M bond orders of 0, 1, and 2, respectively, as has previously been claimed and (2) how do the electronic structures of the $X_4W_2(\mu\text{-}CSiMe_3)_2$ molecules differ as a function of X = $Me_3SiCH_2$ vs. RO. In an attempt to address these questions, we have carried out MO calculations employing both the extended Hückel and Fenske–Hall methods and examined the gas-phase photoelectron spectra of related tantalum and tungsten compounds.

**EHMO Modeling of $M_2(\mu\text{-}CSiMe_3)_2(CH_2SiMe_3)_4$ (M = Ta, W, Re).** Calculations were performed on an idealized $W_2(\mu\text{-}CH)_2H_4^x$ molecule/ion having $D_{2h}$ symmetry as a model for the compounds $(Me_3SiCH_2)_4M_2(\mu\text{-}CSiMe_3)_2$ (M = Ta, $x$ = 2+; M = W, $x$ = 0; M = Re, $x$ = 2–). To ensure that consistent energy values were obtained from the calculations, tungsten parameters were used in all three molecules, while the atomic coordinates and molecular charges were varied to model to the Ta, W, and Re molecules. The atomic coordinates derived from the structural parameters of the Nb,[17] W,[19] and Re[20] complexes are summarized in Table V, and previously published atomic parameters were used for W.[25]

The results of the calculation on $W_2(\mu\text{-}CH)_2H_4$, are shown in Figure 2. The Ta and Re model calculations had similar general MO patterns. The $a_g$ symmetry HOMO of $W_2(\mu\text{-}CH)_2H_4$ has >90% W d character and shows a strong W–W $\sigma$-bonding interaction. The LUMO is predicted to be a W–W $\delta^*$ orbital of $a_u$ symmetry. It should

(22) Fanwick, P. E.; Ogilvey, A. E.; Rothwell, I. P. *Organometallics* **1987**, *6*, 73.
(23) Cotton, F. A.; Schwotzer, W.; Shamshoum, E. S. *Organometallics* **1983**, *2*, 1167.
(24) For a list of distances for related Mo(V) dimers bridged by oxo ligands, $Mo_2(\mu\text{-}O)_2$, see: Chisholm, M. H.; Folting, K.; Kirkpatrick, C. C.; Huffman, J. C. *Inorg. Chem.* **1984**, *23*, 1021.
(25) Summerville, R. H.; Hoffmann, R. *J. Am. Chem. Soc.* **1979**, *101*, 3821.

**Table II. Valence Photoelectron Ionization Band Characteristics[a]**

| compd | band | position, eV | half-width high | half-width low | rel area |
|---|---|---|---|---|---|
| $W_2(\mu\text{-}CSiMe_3)_2(O\text{-}i\text{-}Pr_4)$ | I | 6.18 | 0.58 | 0.48 | 1.0 |
| | II | 7.30 | 0.40 | 0.36 | 1.0 |
| | II′ | 7.96 | 0.90 | 0.55 | 3.4 |
| $W_2(\mu\text{-}CSiMe_3)_2(CH_2SiMe_3)_4$ | I | 6.54 | 0.56 | 0.55 | 1.0 |
| | II | 7.96 | 0.73 | 0.51 | 4.2 |
| $Ta_2(\mu\text{-}CSiMe_3)_2(CH_2SiMe_3)_4$ | II | 7.73 | 0.53 | 0.56 | |

[a] Bands were fit with asymmetric Gaussian functions as described previously.[28] The high half-width is the Gaussian width parameter indicated by the high binding energy side of the band. The total half-width is the average of the high and the low widths.

be noted that the small HOMO/LUMO gap predicted for $W_2(\mu\text{-}CH)_2H_4$ is evidently an artifact of the EHMO calculation and is not supported by the observation of very low-energy absorption bands or anomalous magnetic or NMR behavior for $W_2(\mu\text{-}CSiMe_3)_2(CH_2SiMe_3)_4$.

Variations in M–M bond distances in the Ta, W, and Re complexes can be explained by comparing the occupations of the $a_g$ and $a_u$ orbitals throughout the series. The LUMO for $W_2(\mu\text{-}CH)_2H_4^{2+}$ is the $a_g$ orbital, predicting accurately that the Ta complex has no direct M–M bond. The HOMO for $W_2(\mu\text{-}CH)_2H_4^{2-}$ is not a M–M $\pi$ orbital as was originally proposed[20] but is the M–M $\delta^*$ $a_u$ orbital. The $\sigma^2\delta^{*2}$ M–M bonding configuration predicted by the calculation successfully explains why the Re–Re distance is 0.02 Å longer than the M–M distance found in its $\sigma^2$-bonded W analogue.

An envelope of four orbitals, which have at least 50% carbon character, appears at approximately 2 eV below the $a_g$ orbital in each of the model calculation. This group of orbitals is spread over approximately 1 eV. Two of the orbitals, having $b_{3g}$ and $b_{2u}$ symmetry, form two of the four M–$\mu$-C $\sigma$ bonds. The remaining two orbitals have $b_{2g}$ and $b_{3u}$ symmetry and represent the in- and out-of-phase components of the M–$\mu$-C $\pi$ bonds.

**Fenske–Hall Calculations on $M_2(\mu\text{-}CH)_2(CH_3)_4$ (M = Ta, W, Re).** In order to develop an independent check of the results from EHMO calculations, Fenske–Hall MO calculations[21,26] were performed on models of the $M_2(\mu\text{-}CSiMe_3)_2(CH_2SiMe_3)_4$ molecules.

The results of the FHMO calculations are summarized in the orbital diagram in Figure 3 and show only four minor differences from the MO picture determined through extended Hückel calculations. (1) The HOMO/LUMO gap for $W_2(\mu\text{-}CH)_2(CH_3)_4$ is predicted to be approximately 2 eV, much more substantial than the 0.5 eV predicted by EHMO calculations. (2) The next orbital below the $6a_g$ M–M $\sigma$ bond is found to be the in-phase component of the W–$\mu$-C $\pi$ bond, the $4b_{3u}$ orbital, throughout the Ta, W, and Re model series. (3) The envelope of four orbitals containing two W–$\mu$-C $\sigma$ and two W–$\mu$-C $\pi$ bonds found within a 1-eV region in the EHMO calculation is spread over a 3-eV range in the Fenske–Hall calculation. (4) The $5a_g$ orbital, which is another component of the W–$\mu$-C $\sigma$ bond, appears at higher energy in the FHMO calculation intruding into the envelope of four $\sigma$- and $\pi$-bonding orbitals mentioned above.

**UV Photoelectron Spectra of the 1,3-Dimetallacyclobutadienes.** Helium I PE spectra of the tantalum and tungsten compounds were obtained by previously published procedures.[27-31] The upper valence regions (IP's

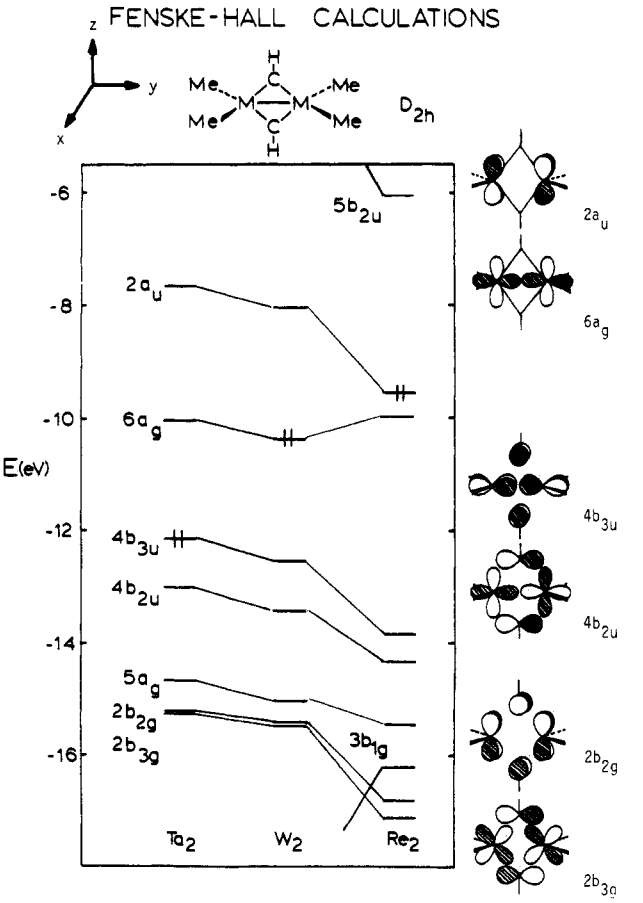


**Figure 3.** Results of the Fenske–Hall MO calculations on $M_2(\mu\text{-}CH)_2(CH_3)_4$ (M = Ta, W, or Re). The $5a_g$ and $3b_{1g}$ orbitals, which are not shown in the drawings, are the remaining two orbitals in the set of four that comprise the W–C $\sigma$ bonds. These orbitals fall at a much lower relative energy in the EHMO calculations.

< 12 eV) are shown in Figure 4, and characteristics of the resolved ionization bands are given in Table II. The spectra can be divided into four regions representing ionizations from distinct types of bonding orbitals that are now discussed.

All three spectra show an intense, essentially featureless band between 9.5 and 11 eV. For the $M_2(CSiMe_3)_2(CH_2SiMe_3)_4$ species, this band can be assigned to ionizations from the C–Si bonds.[32,33] For the $W_2(CSiMe_3)_2$(O-

(26) Bursten, B. E.; Jensen, J. R.; Fenske, R. F. *J. Chem. Phys.* **1978**, *68*, 3320.
(27) Calabro, D. C.; Hubbard, J. L.; Blevins, II, C. H.; Campbell, A. C.; Lichtenberger, D. L. *J. Am. Chem. Soc.* **1981**, *103*, 6739.
(28) Lichtenberger, D. L.; Calabro, D. C.; Kellogg, G. E. *Organometallics* **1984**, *3*, 1623.
(29) Hubbard, J. L. *Diss. Abstr. Int. B* **1983**, *43*, 2203.
(30) Kellogg, G. E. *Diss. Abstr. Int. B* **1986**, *46*, 3838.
(31) Lichtenberger, D. L.; Kellogg, G. E.; Kristofzski, J. G.; Page, D.; Turner, S.; Klinger, G.; Lorenzen, J. *Rev. Sci. Instrum.* **1986**, *57*, 2366.
(32) Evans, A.; Green, J. C.; Joachim, P. J.; Orchard, A. F.; Turner, D. W.; Maier, J. P. *J. Chem. Soc., Faraday Trans.* **1972**, *68*, 905.
(33) Lappert, M. F.; Pedley, J. B.; Sharp, G. *J. Organomet. Chem.* **1974**, *66*, 271.

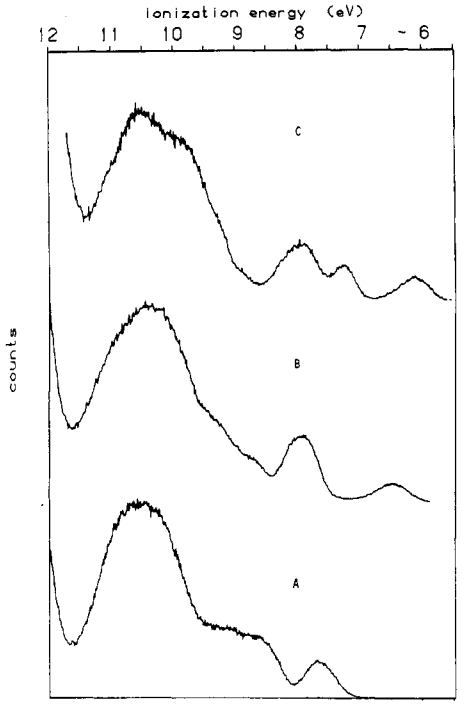


**Figure 4.** HeI valence photoelectron spectra of (A) $Ta_2(\mu\text{-}CSiMe_3)_2(CH_2SiMe_3)_4$, (B) $W_2(\mu\text{-}CSiMe_3)_2(CH_2SiMe_3)_4$, and (C) $W_2(\mu\text{-}CSiMe_3)_2(O\text{-}i\text{-}Pr)_4$.

$i\text{-}Pr)_4$, this band contains ionizations from the oxygen lone-pair electrons.[34] Ionizations from metal–terminal alkyl $\sigma$ bonds typically occur between 8.5 and 9.5 eV,[33,35] and such an assignment appears reasonable for the present set of complexes. The relative lack of intensity at 8.5–9.0 eV for the alkoxide complex is consistent with this assessment. Some ionizations from the 1,3-$M_2C_2$ $\sigma$ and $\pi$ bonds probably also occur in this region. The ionization bands that occur between 7.0 and 8.5 eV can probably all be attributed as being from the 1,3-$M_2C_2$ $\sigma$ and $\pi$ bonds since this would be a somewhat low energy for "normal" M–C $\sigma$-bond ionizations. (There is undoubtedly some mixing between the two types of orbitals.) Finally, the ionization for the two W complexes that occurs at 6–6.5 eV, which is absent in the Ta complex, can be assigned to the $6a_g$ W–W $\sigma$-bonding orbital.

A contour plot of the $6a_g$ orbital from one of the Fenske–Hall calculations is shown in Figure 5. The $6a_g$ orbital shows significant overlap between the W centers and has only a small amount of W–C character. The ionizations from this orbital are quite broad, indicating that the W–W distance increases significantly upon the removal of an electron from the W–W bond.

The ionization features between 7.0 and 8.5 eV exhibit interesting differences for the three complexes. For the Ta complex, the band at 7.7 eV certainly represents the ionization from the $4b_{3u}$ orbital that is calculated to be the HOMO. A close-up view of this ionization shows a slight asymmetry on the low-energy side. (Note the fit parameters in Table II where the low-energy-side half-width is greater than that of the high-energy side.) This suggests that two ionization processes may be present in this first

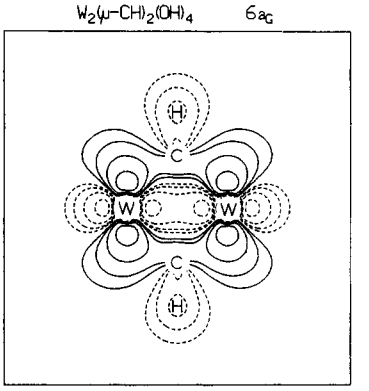


**Figure 5.** Contour plot of the $6a_g$ W–W $\sigma$-bonding orbital derived from the Fenske–Hall MO calculation on $W_2(\mu\text{-}CH)_2(OH)_4$. The plot shows the molecular plane containing the $W_2(\mu\text{-}CH)_2$ core unit.

band; a likely assignment for the second ionization suggested by the FHMO calculation would be from the $4b_{2u}$ orbital.

The comparison of the W and Ta analogues is rather intriguing. Scaled vs. the C-Si ionization intensity, the ionization at 8.0 eV in the W complex is about twice as intense as the ionization at 7.7 eV in the Ta complex. Also there is decreased intensity at 8.5–9.0 eV in the W relative to the Ta complex. This suggests that at least one orbital is substantially destabilized upon the Ta to W transformation and that the band at 8.0 eV in the W species represents at least two ionization processes. Consistent with this is that the band is not well fit by a single asymmetric Gaussian (note the large disparity in the halfwidths listed in Table II). Unfortunately, the FHMO calculations provide no clues to the identity of this orbital(s) that shifts upon the W for Ta substitution. However, the FHMO calculation does suggest that at least ionizations from the $4b_{3u}$ and $4b_{2u}$ orbitals are present in the band at 8.0 eV in the W complex.

The replacement of the four alkyl ligands by four alkoxide ligands in the W species gives rise to further interesting changes in the spectra. The single broad band at 8.0 eV in the alkyl species is apparently split into two ionizations at 7.2 and 8.0 eV in the alkoxide species. From Table II, it is seen that the total area of these two ionizations of the alkoxide species (relative to the first ionization band) is roughly equal to that of the single band of the alkyl species. This suggests that ionization at 7.2 eV in the alkoxide species corresponds to one of the ionizations present in the 8.0-eV band of the alkyl species rather than some higher lying ionization. The large asymmetry of the 8.0-eV ionization band of the alkoxide species (see Table II) is again suggestive of the presence of more than one ionization process. Because of their close correspondence, it is presumed that whatever orbital ionizations are present in the 8.0-eV band of the alkoxide species are also represented in the 8.0-eV band of the alkyl species. The unique destabilization of orbitals represented by the 7.2-eV band of the alkoxide complex is probably attributable to $\pi$ interactions with the alkoxide ligands that would not be present in the alkyl species. In an effort to further characterize such an interaction, we compared the electronic structures of the two W complexes via FHMO calculations.

**Fenske–Hall MO Calculations on $W_2(\mu\text{-}CH)_2(OH)_4$.** Molecular coordinates for the $W_2(\mu\text{-}CH)_2(OH)_4$ model used in this calculation were derived from the structure of $(i\text{-}PrO)_4W_2(\mu\text{-}CSiMe_3)_2$[1] and are listed in Table V. Hydroxide ligands in the model were arranged to retain $D_{2h}$ symmetry.

(34) (a) Cotton, F. A.; Stanley, G. G.; Kalbacher, B. J.; Green, J. C.; Seddon, E.; Chisholm, M. H. *Proc. Natl. Acad. Sci. U.S.A.* **1977**, *74*, 3109. (b) Bursten, B. E.; Cotton, F. A.; Green, J. C.; Seddon, E. A.; Stanley, L. L. *J. Am. Chem. Soc.* **1980**, *102*, 4579. (c) Kober, E. M.; Lichtenberger, D. L. *J. Am. Chem. Soc.* **1985**, *107*, 7199.

(35) (a) Gaylor, L.; Wilkinson, G.; Lloyd, D. R. *J. Chem. Soc., Chem. Commun.* **1975**, 497. (b) Green, J. C.; Jackson, S. E.; Higginson, B. *J. Chem. Soc., Dalton Trans.* **1975**, 403.

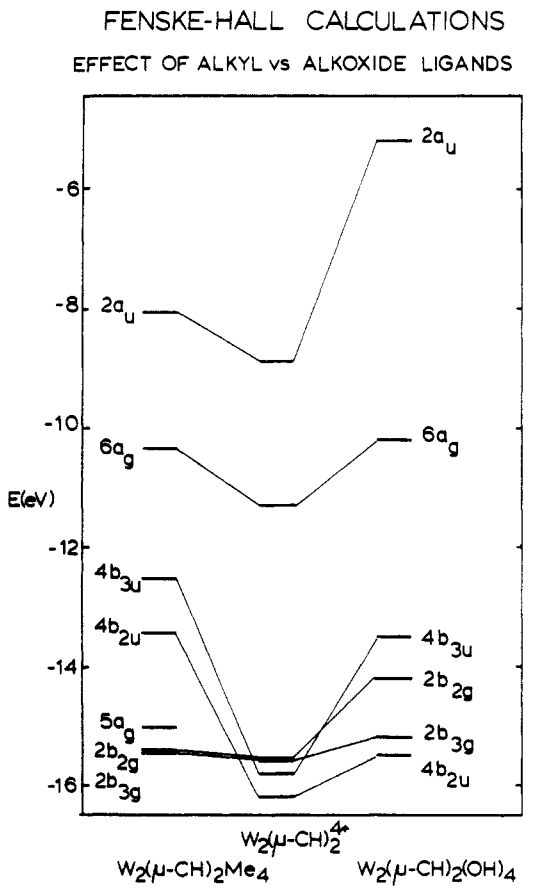


**Figure 6.** Results of Fenske–Hall MO calculations comparing $W_2(\mu\text{-}CH)_2X_4$ (X = $CH_3$ or OH).

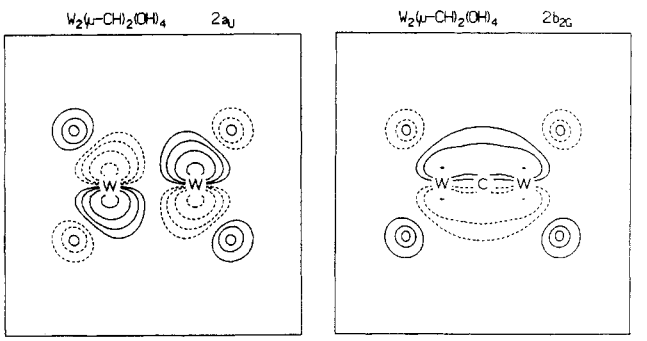


**Figure 7.** Contour plot of the $2a_u$ and $2b_{2g}$ orbitals of $W_2(\mu\text{-}CH)_2(OH)_4$ showing $\pi^*$ interactions between W-based $d\pi$-orbital fragments and $p\pi$ fragments on the terminal OH ligands. The plot is parallel to the $x,y$ plane which contains the $W_2(OH)_4$ atoms.

The diagrams shown in Figure 6 are a comparison of the molecular orbital energies of the $M_2(CH)_2^{4+}$ core unit and two identical core systems bearing terminal methyl and hydroxide ligands, respectively. The calculations predict a large increase in the HOMO/LUMO gap for the hydroxide-substituted molecule because the $2a_u$ LUMO appears at much higher energy in $W_2(\mu\text{-}CH)_2(OH)_4$ than in $W_2(\mu\text{-}CH)_2(CH_3)_4$. The contour plot of the $\delta^*$ orbital in $W_2(\mu\text{-}CH)_2(OH)_4$, shown in Figure 7, demonstrates that the predicted destabilization is due to an antibonding interaction between the metal $\delta^*$ fragment and a small component of a p* orbital of $a_u$ symmetry localized on the hydroxide oxygens.

The $2b_{2g}$ orbital, which is the out-of-phase component of the W–$\mu$-C $\pi$ bond having a small $\delta$-bonding $W_2$ component, is also strongly destabilized in $W_2(\mu\text{-}CH)_2(OH)_4$. As is shown in the contour plot in Figure 7, the $2b_{2g}$ orbital is again destabilized by an antibonding interaction between the metal $\delta$ fragment and a $p\pi$ orbital of $b_{2g}$ symmetry localized on the hydroxide oxygens. The $2b_{2g}$ orbital is not destabilized as strongly as the $2a_u$ orbital, however, because it has a smaller overall percentage of metal character. In reality, the effect of this antibonding mixing may push the $2b_{2g}$ orbital to even higher energy than is predicted by the FHMO calculation, forcing it to lie somewhat above the $4b_{3u}$ orbital in the energy diagram shown in Figure 6. This would lead us to predict that the peak at 7.2 eV in the PE spectrum of $W_2(\mu\text{-}CSiMe_3)_2(O\text{-}i\text{-}Pr)_4$ is due to an ionization from the $2b_{2g}$ orbital.

The final significant difference between the valence electronic structures of the alkoxide- and alkyl-substituted derivatives is that the alkoxide ligands are slightly more destabilizing toward the $6a_g$ W–W $\sigma$-bonding orbital. This effect is visible in the PE spectra of the W compounds, which show $6a_g$ ionizations from the alkyl- and alkoxide-substituted molecules at 6.5 and 6.15 eV, respectively. In addition, a Mulliken population analysis of the $6a_g$ orbital of $W_2(\mu\text{-}CH)_2(CH_3)_4$ demonstrated that the W–W overlap is greater at a 2.54 Å intermetallic distance than at 2.62 Å. The opposite trend is observed for the hydroxide-substituted derivative. These overlap trends agree with the consistent observation of longer W–W bonds in alkoxide-substituted ditungstacyclobutadiene derivatives. The reduced bonding in the $6a_g$ orbital of the alkoxide is also evident in the slightly narrower half-width of this ionization.

It is also interesting that the W–$\mu$-C distances increase slightly (0.03 Å) upon the alkoxide for alkyl substitution. Since the $2b_{2g}$ orbital is M–$\mu$-C $\pi$ bonding, its destabilization by an antibonding $\pi$ interaction with the alkoxide ligands would weaken the M–C $\pi$ bonding. (This shows up in the W–$\mu$-C overlap population.) The interaction between the alkoxide ligands and the $2a_u$ orbital does not effect this however, since the $2a_u$ orbital is nonbonding between W and $\mu$-C. The latter interaction strengthens the M–O bond by providing a $\pi$ bond, and its presence necessitates the antibonding interaction with the $2b_{2g}$ orbital.

Finally it is worth noting that the substitution of two $Me_3SiCH_2$ ligands by phenoxides, $OC_6H_2$-2,4,6-$t$-$Bu_3$, has a minimal effect on the $Ta_2(\mu\text{-}C)_2$ core in the related $d^0$–$d^0$ compounds.[22] No change in M–M distance is understandable because the M–M $\sigma$ orbital is not occupied. The effect of phenoxide substitution on M–C $\pi$ bonding and M–C distances is probably very small because phenoxy groups are weaker $\pi$ donors than alkoxides.

**Table III. UV/Visible Spectra Data for Some 1,3-Dimetallacyclobutadienes**

| compd | $\lambda_{max}$, nm | $\epsilon$, $M^{-1}$ $cm^{-1}$ |
|---|---|---|
| $Ta_2(\mu\text{-}CSiMe_3)_2(CH_2SiMe_3)_4$ | 409 | 4600 |
| | 306 | 6800 |
| $W_2(\mu\text{-}CSiMe_3)_2(CH_2SiMe_3)_4$ | 377 | 5600 |
| | 304 | 4900 |
| $W_2(\mu\text{-}CSiMe_3)_2(O\text{-}i\text{-}Pr)_4$ | 375 | 6400 |
| | 354 | 7200 |
| | 273 | 8000 |
| | 249 | 12300 |

[a] Hexane solutions.

**Discussion of the UV/Visible Spectra.** UV/visible absorption spectra of the ditantalum and ditungsten compounds covering the range 220–500 nm are collected in Table III. It seems puzzling that the spectra of the Ta and W derivatives should appear so similar in spite of the absence of a M–M $\sigma$ bond in the tantalum complex. Although absolute assignments of energies to transitions between various electronic states are not possible on the

basis of the simple calculations performed in this study, we can use symmetry arguments to determine which transitions might occur and to develop qualitative explanations for the observed spectra.

In a $D_{2h}$ point group, the following electronic transitions originating in the valence orbitals of the $Ta_2(\mu\text{-}CH)_2H_4$ model are symmetry allowed:

$$b_{3u}(\text{HOMO}) \rightarrow a_g(\text{LUMO}) \quad \text{i}$$

$$b_{2u} \rightarrow a_g(\text{LUMO}) \quad \text{ii}$$

$$b_{2g} \rightarrow a_u(\text{SLUMO}) \quad \text{iii}$$

$$b_{3g} \rightarrow a_u(\text{SLUMO}) \quad \text{iv}$$

These transitions can logically be divided into two groups: transitions from the $b_{3u}$ and $b_{2u}$ orbitals to the $a_g$ LUMO should require smaller amounts of energy than transitions from the $b_{2g}$ and $b_{3g}$ orbitals to an $a_u$ SLUMO. The absorption band at 409 nm in the UV/visible spectrum of the Ta complex can be assigned to either one or both of the low-energy transitions to the LUMO, while a similar correlation can be drawn between the high-energy transitions to the SLUMO and the absorption band at 306 nm.

Assuming that these assignments are valid, we must now explain why the spectrum of the related W complex, in which the $a_g$ M–M $\sigma$-bonding orbital is filled, also displays two transitions at 377 and 304 nm. The occupation of the $a_g$ orbital in the W complex has two affects on potential transitions in the 1,3-dimetallacyclobutadiene core. Transitions from the M–$\mu$-C bonding envelope into the $a_g$ orbital, i and ii, are no longer possible, whereas new transitions from the filled $a_g$ orbital to virtual $b_{2u}$ and $b_{3u}$ orbitals are now possible. The transitions from the $b_{2g}$ and $b_{3g}$ orbitals would be unaffected, so the allowed transitions are now:

$$a_g(\text{HOMO}) \rightarrow b_{2u}(\text{SLUMO}) \quad \text{v}$$

$$a_g(\text{HOMO}) \rightarrow b_{3u}(\text{very high lying}) \quad \text{vi}$$

$$b_{2g} \rightarrow a_u(\text{LUMO}) \quad \text{iii}$$

$$b_{3g} \rightarrow a_u(\text{LUMO}) \quad \text{iv}$$

Since the relative energies of the $2b_{2g}$, $2b_{3g}$, and $2a_u$ orbitals are predicted by the FHMO calculation to be essentially unaffected by the Ta–W substitution, the band at 304 nm can be tentatively assigned to transitions iii and iv as for the Ta complex. By elimination, the band at 377 nm is then assigned to v. (On the basis of the relative orbital energies from the FHMO, v is estimated to occur at a lower energy than iii or iv.)

The absorption spectrum of $(i\text{-PrO})_4W_2(\mu\text{-}CSiMe_3)_2$ has four maxima in the UV region in spite of having the same symmetry, and consequently the same symmetry-allowed transitions, as its structural analogue $(Me_3SiCH_2)_4W_2(\mu\text{-}CSiMe_3)_2$. With the aid of the FHMO calculation, some tentative assignments can be proposed. The relative energies of the $6a_g$ and $2b_{2u}$ orbitals are estimated to be relatively unaffected by the alkoxide–alkyl substitution, so the band at 375 nm could be assigned to v as with the alkyl complex. The $b_{2g}$ and $b_{3g}$ orbitals are calculated to be substantially split in the alkoxide complex whereas they appear to be nearly isoenergetic for the alkyl species. Thus, transitions iii and iv should be well-resolved and might be assigned to the 354- and 273-nm bands, respectively. The greater strengths of these bands relative to the 304-nm band of the alkyl species argues against such an assignment, but there is much overlapping of bands in the alkoxide species so true intensities are difficult to judge. The intense band at 249 nm is unique to the alkoxide species and so probably has a different origin than the other bands. A reasonable assignment would be $O(p\pi)(b_{2g},b_{3g})$ to $W(a_u)$ ligand to metal charge transfer.

All of the above assignments must be viewed as tentative since polarization or similar supportive data is lacking. Also, more sophisticated techniques than the FHMO method would be helpful in justifying the assignments. However, the observed patterns do seem to be reasonably well accounted for.

**Electronic Structure and Reactivity of the $M_2(\mu\text{-}CR)_2$ Core.** Our studies of the electronic structure of the $M_2(\mu\text{-}CR)_2X_4$ derivatives have helped to clarify the origin of various structural changes in the $M_2(\mu\text{-}CR)_2$ core system. There remain two major correlations between chemical reactivity and electronic structure that should be examined; first the relationship between M–M bond order and the stability of the ligand adducts of structure II, and second, the different activation energies encountered for similar chemical processes at $W_2(\mu\text{-}CSiMe_3)_2$ centers bearing terminal alkoxide or alkyl ligands.

**The Effect of M–M Bond Order on Adduct Formation.** The presence or absence of a M–M bond has a drastic effect on the stability of ligand adducts of the $M_2(\mu\text{-}CSiMe_3)_2X_4$ molecules. While no stable tantalum adducts have been observed, complexes between the tungsten compounds and alkynes, allenes, and aryldiazomethanes have all been isolated or spectroscopically observed.[16] In addition, structural data suggest that these ligands act as $\pi$ acceptors, heterolytically cleaving the M–M bond upon coordination.

This process can be understood by considering the MO symmetry at the site of ligand attack. The incoming ligand (Y) probably approaches one of the W centers trans to the metal–carbon bond of one of the $\mu$-alkylidyne ligands, which is the position it ultimately occupies in the fully formed complex. Along any of these four vectors, the $6a_g$ HOMO of the $W_2(\mu\text{-}CR)_2$ core unit has $\pi$ symmetry. Consequently, this orbital can readily overlap with an unfilled $\pi^*$ orbital on Y, forming the W–Y $\pi$ bond with concurrent disruption of the W–W $\sigma$ bond. The metal–ligand bonds developed from $\sigma$ donation by Y and d$\pi$ back-donation by the metal stabilizes the $W_2$:Y complex far more than isostructural Ta complex in which only the $\sigma$-donor component can participate.

**Effects of Terminal Ligands on Reactions at the $W_2(\mu\text{-}CR)_2$ Unit.** The activation parameters for the insertion of allenes and alkynes into a $\mu$-$CSiMe_3$ ligand in $W_2(\mu\text{-}CSiMe_3)_2(O\text{-}i\text{-}Pr)_4$ are different than those observed for $W_2(\mu\text{-}CSiMe_3)_2(CH_2SiMe_3)_4$. In fact, the rate of allene insertion, $k_{obsd}$, is directly dependent on the number of $\pi$-donor alkoxide ligands on each metal center: I > $W_2(\mu\text{-}CSiMe_3)_2(O\text{-}t\text{-}Bu)_2(CH_2SiMe_3)_4$ > $W_2(\mu\text{-}CSiMe_3)_2(O\text{-}i\text{-}Pr)_4$.[12] A possible explanation for this behavior is that the alkoxide ligands compete with Y for access to W d$\pi$ orbitals, thereby destabilizing the adduct III. Stating this effect differently, since $\pi$-donor orbitals on both Y and the alkoxide ligands must mix with the same metal d orbitals in $W_2(\mu\text{-}CSiMe_3)_2(O\text{-}i\text{-}Pr)_4$, the resulting M–Y $\pi$ bonds are energetically destabilized as compared with similar bonds in $W_2(\mu\text{-}CSiMe_3)_2(CH_2SiMe_3)_4$. The stability order for Y is Y = $Ph_2CN_2 \gg RC{\equiv}CR >$ allene that is the same for supporting $Me_3SiCH_2$ and OR ligands and reflects the $\pi$-donating ability of Y.

Various fluxional processes of the alkoxide-substituted ditungstacyclobutadiene derivatives have consistently higher activation energies than their alkyl-substituted analogues.[1] Alkoxide-induced destabilization of virtual

orbitals used in these rearrangement processes could account for these differences.

## Concluding Remarks

Combining the results of EHMO and FHMO calculations with spectroscopic investigations of the $M_2(\mu\text{-}CSiMe_3)_2X_4$ molecules has allowed us to develop an extensive picture of the valence electronic structure of the dimetallacyclobutadiene unit. The prediction of a $\sigma^2\delta^{*2}$ M–M bonding configuration for $Re_2(\mu\text{-}CSiMe_3)_2(CH_2SiMe_3)_4$ provides the first adequate explanation for its long Re–Re bond distance. The shape of the $6a_g$ W–W $\sigma$-bonding HOMO in I explains why I reacts readily with a variety of unsaturated organic substrates that show no reaction with the isostructural Ta derivative. Terminal alkoxide ligands on the $W_2$ core unit exert their strongest destabilizing influence on orbitals with $\delta$ or $\delta^*$ character, evidently because these W orbitals are suitably directed to maximize $d\pi$–$p\pi$ overlap. Although the presence of alkoxide ligands increases the activation energies for a variety of reactions and fluxional processes that occur on the $W_2(\mu\text{-}CSiMe_3)X_4$ template, it is currently unclear whether this effect is solely due to the destabilization of $\delta$-type metal orbitals or whether it involves more complex $\pi$-bonding interactions. Further elaboration of these processes will require detailed theoretical examinations of individual rearrangement and insertion reactions.

## Experimental Section

All solids were isolated and transferred in a dry $N_2$-filled Vacuum Atmospheres glovebox. Solvents and liquid reactants were transferred via syringe, while filtrations and other manipulations of reaction mixtures were accomplished by double Schlenk techniques.

Solvents were dried and deoxygenated by refluxing under dry $N_2$ gas over sodium benzophenoneketyl except for $CH_3CN$ which was distilled from $P_2O_5$ and then from $CaH_2$. Alcohols were dried by refluxing over Mg turnings. NMR solvents were dried over 3-Å molecular sieves and deoxygenated with a dry $N_2$ purge. $^1H$ and $^{13}C$ NMR spectra were acquired on Nicolet 360 and Varian XL-300 FT spectrometers, respectively. Chemical shifts were referenced against either the residual $^1H$ impurity in benzene-$d_6$ (7.15 ppm) or the methyl group of toluene-$d_8$ (2.09 ppm). $^{13}C$ chemical shifts were referenced against the methyl carbon nucleus of toluene-$d_8$ (20.5 ppm). UV spectra were acquired in hexanes and pentanes solvents by using 10-mm and 1.0-mm path length cells on a Perkin-Elmer 330 UV/vis spectrophotometer over a scan range from 800 to 220 nm. Analytical data were obtained from Microanalytical Laboratories, Engelskirchen, FRG. All samples were ignited with $V_2O_5$ due to silicon content.

**Photoelectron Spectra.** The photoelectron spectra were measured on a spectrometer with specially designed photon sources, ionization cells, 36-cm radius hemispherical analyzer (McPherson), power supplies, counter interface, and collection methods that have been described elsewhere.[27-31] The spectra were measured with the sample ionization cell at 90–100 °C. The argon ionization at 15.759 eV was used as an internal calibration lock of the energy scale.

$W_2(\mu\text{-}CSiMe_3)_2(CH_2SiMe_3)_4$ (I), $W_2(\mu\text{-}CSiMe_3)_2(O\text{-}i\text{-}Pr)_4$, and $Ta_2(\mu\text{-}CSiMe_3)_2(CH_2SiMe_3)_4$ were prepared according to previously published procedures.[16,17]

**Synthesis of $W_2(\mu\text{-}CSiMe_3)_2(O\text{-}t\text{-}Bu)_2(CH_2SiMe_3)_2$.** $W_2(\mu\text{-}CSiMe_3)_2(CH_2SiMe_3)_4$ (1.5 mmol) was added to a Schlenk flask (25 mL), and $t$-BuOH/benzene azeotrope (5 mL) was added to the flask via syringe. After the mixture was left standing overnight at ambient temperature, the solvents were removed under a dynamic vacuum, the yellow-brown residue was dissolved in hexanes (5 mL), and the resulting solution was filtered. The hexanes were removed in vacuo. A $^1H$ NMR spectrum of the solid residues suggested the presence of two isomers of $W_2(\mu\text{-}CSiMe_3)_2(O\text{-}t\text{-}Bu)_2(CH_2SiMe_3)_2$ in a 5:3 ratio. A sample of the crude product mixture (600 mg) was dissolved in a mixture of hexanes (1.2 mL) and toluene (0.40 mL) and was placed in a refrigerator at −20 °C. After 4 days a crop of beautiful orange-yellow microcrystals formed (140 mg). The mother liquor was removed via syringe; the crystals were dried in vacuo and were identified as the minor isomer of $W_2(\mu\text{-}CSiMe_3)_2(CH_2SiMe_3)_2(O\text{-}t\text{-}Bu)_2$ by $^1H$ and $^{13}C$ NMR spectroscopy and elemental analysis. Yield: 23%. Anal. Calcd: C, 33.41; H, 7.19. Found: C, 33.27; H, 6.60. Minor isomer: $^1H$ NMR data (benzene-$d_6$, 23 °C) $\delta$ 1.03 (18 H, s, $OCMe_3$), 0.56 (18 H, s, $CH_2SiMe_3$), 0.45 (18 H, s, $\mu$-$CSiMe_3$), −0.75 (4 H, s, $CH_2SiMe_3$); $^{13}C$ NMR data (toluene-$d_8$, 23 °C) $\delta$ 324.1 ($J_{^{13}C-^{183}W}$ = 124.7 Hz, $\mu$-$CSiMe_3$), 81.3 ($OCMe_3$), 48.6 ($J_{^{13}C-^{183}W}$ = 93.5 Hz, $CH_2SiMe_3$), 32.7 ($OCMe_3$), 3.1 and 2.1 ($CH_2SiMe_3$, $\mu$-$CSiMe_3$). Major isomer: $^1H$ NMR data (benzene-$d_6$, 23 °C) $\delta$ 1.11 (18 H, s, $OCMe_3$), 0.51 (18 H, s, $\mu$-$CSiMe_3$), 0.39 (18 H, s, $CH_2SiMe_3$), −0.80 (4 H, s, $CH_2SiMe_3$).

**Table IV. Bond Distances (Å) and Bond Angles (deg)**

| | | | |
|---|---|---|---|
| | $Ta_2(\mu\text{-}CH)_2$ | | |
| Ta–Ta | 2.896 | Ta–Ta–C | 47.2 |
| Ta–C | 1.97 | Ta–C–H | 137.2 |
| C–H | 1.09 | | |
| | $W_2(\mu\text{-}CH)_2$ (Short W–W Distance) | | |
| W–W | 2.54 | W–W–C | 48 |
| W–C | 1.89 | W–C–H | 138 |
| CH | 1.09 | | |
| | $W_2(\mu\text{-}CH)_2$ (Long W–W Distance) | | |
| W–W | 2.62 | W–W–C | 48 |
| W–C | 1.95 | W–C–H | 138 |
| C–H | 1.09 | | |
| | $Re_2(\mu\text{-}CH)_2$ | | |
| Re–Re | 2.55 | W–W–C | 41.5 |
| Re–C | 1.92 | W–C–H | 131.5 |
| C–H | 1.09 | | |

**Table V. Atomic Coordinates**

| atom | $x$ | $y$ | $z$ |
|---|---|---|---|
| | $W_2(\mu\text{-}CH)_2(CH_3)_4$ (Long W–W Distance) | | |
| W(1) | 0.000 00 | 1.311 00 | 0.000 00 |
| W(2) | 0.000 00 | −1.311 00 | 0.000 00 |
| C(3) | 0.000 00 | 0.006 20 | 1.449 13 |
| C(4) | 0.000 00 | −0.006 20 | −1.449 13 |
| H(5) | 0.000 00 | 0.006 20 | 2.539 13 |
| H(6) | 0.000 00 | −0.006 20 | −2.539 13 |
| C(7) | 1.752 82 | 2.449 29 | 0.000 00 |
| C(8) | −1.752 82 | 2.449 29 | 0.000 00 |
| C(9) | 1.752 62 | −2.449 30 | 0.000 00 |
| C(10) | −1.752 82 | −2.449 30 | 0.000 00 |
| H(11) | 2.611 75 | 1.778 28 | 0.000 00 |
| H(12) | 1.769 78 | 3.074 74 | −0.892 54 |
| H(13) | 1.769 78 | 3.074 74 | 0.892 54 |
| H(14) | −2.611 75 | 1.779 22 | 0.000 00 |
| H(15) | −1.769 78 | 3.074 74 | −0.892 54 |
| H(16) | −1.769 78 | 3.074 74 | 0.892 54 |
| H(17) | 2.611 75 | −1.778 22 | 0.000 0 |
| H(18) | 1.769 78 | −3.074 74 | 0.892 54 |
| H(19) | 1.769 78 | −3.074 75 | −0.892 54 |
| H(20) | −2.611 75 | −1.778 22 | 0.000 00 |
| H(21) | −1.769 78 | −3.074 75 | 0.892 54 |
| H(22) | −1.769 78 | −3.074 74 | −0.592 54 |
| | $W_2(\mu\text{-}CH)_2(OH)_4$ (Long W–W Distance) | | |
| W(1) | 0.000 00 | 1.311 00 | 0.000 00 |
| W(2) | 0.000 00 | −1.311 00 | 0.000 00 |
| C(3) | 0.000 00 | 0.006 20 | 1.449 13 |
| C(4) | 0.000 00 | −0.006 20 | −1.449 13 |
| H(5) | 0.000 00 | 0.006 20 | 2.539 13 |
| H(6) | 0.000 00 | −0.006 20 | −2.539 13 |
| O(7) | 1.551 54 | 2.318 58 | 0.000 00 |
| H(8) | 2.490 56 | 2.518 17 | 0.000 00 |
| O(9) | −1.551 54 | 2.318 58 | 0.000 00 |
| H(10) | −2.490 56 | 2.518 17 | 0.000 00 |
| O(11) | 1.551 54 | −2.318 58 | 0.000 00 |
| H(12) | 2.490 56 | −2.518 18 | 0.000 00 |
| O(13) | −1.551 54 | −2.318 58 | 0.000 00 |
| H(14) | −2.490 56 | −2.518 18 | 0.000 00 |

**Molecular Orbital Calculations.** EHMO calculations were performed on an CDC Cyber 7600 using the ICON subroutine and previously published atomic parameters. Variations in the W–W bond distances of $W_2(\mu\text{-}CH)_2H_4$ and $W_2(\mu\text{-}CH)_2(OH)_4$ caused a smooth decrease in W–W overlap with increasing internuclear distance.

Fenske–Hall MO calculations were performed on a VAX/1170 computer system. Atomic basis functions for Ta(I), W(I), and Re(I) were calculated by Herman–Skillman atomic calculations according to the method of Bursten, Fenske, and Jensen[27] using fixed 6s and 6p exponents and contracted double-$\zeta$ representations for the W 5d AO's. Calculations were converged to a population agreement of 0.001. Metal basis functions were derived by using 6s exponents fixed at 1.8 and 6p exponents of 1.6, 1.8, and 2.0 for Ta, W, and Re, respectively. A 1s exponent of 1.16 was used for the H atom. The skeletal coordinates used in the $M_2(\mu\text{-}CH)_2(CH_3)_4$ models of the Ta, W, and Re derivatives were identical with those listed in Table V and the four terminal methyl groups were oriented to retain $D_{2h}$ symmetry.

**Acknowledgment.** D.L.L. acknowledges support by the U.S. Department of Energy (Division of Chemical Sciences, Office of Basic Energy Sciences, Office of Energy Research, DE-AC02-80ER10746), the National Science Foundation (CHE8519560), and the Materials Characterization Program, University of Arizona. The work at Indiana University was supported by the National Science Foundation and, in part, by the donors of the Petroleum Research Fund, administered by the American Chemical Society.

## Appendix

W–H distances of 1.73 Å and H–W–H angles between 122 and 123° were used in all $W_2(\mu\text{-}CH)_2H_4$ EHMO models. W–O distances of 1.85 Å and W–O–H angles of 159° were used in all $W_2(\mu\text{-}CH)_2(OH)_4$ model calculations.

Distances and angles for the $M_2(\mu\text{-}CH)_2$ unit used in Ta, W, and Re model compounds are listed in Table IV. Representative examples of atomic coordinates for $CH_3$- and OH-substituted model compounds used in FHMO calculations are also listed in Table V.

**Registry No.** $W(\mu\text{-}CSiMe_3)_2(O\text{-}i\text{-}Pr)_4$, 96930-67-5; $W2(\mu\text{-}CSiMe_3)_2(CH_2SiMe_3)_4$, 107201-08-1; $Ta(\mu\text{-}CSiMe_3)_2(CH_2SiMe_3)_4$, 107201-09-2; *syn*-$W2(\mu\text{-}CSiMe_3)_2(CH_2SiMe_3)_2(O\text{-}t\text{-}Bu)_2$, 103238-36-4; *anti*-$W2(\mu\text{-}CSiMe_3)_2(CH_2SiMe_3)_2(O\text{-}t\text{-}Bu)_2$, 103303-26-0; $W2(\mu\text{-}CH)_2H_4$, 107201-10-5; $Ta_2(m\text{-}CH)_2(CH_3)_4$, 107201-11-6; $W2(\mu\text{-}CH)_2(CH_3)_4$, 107201-12-7; $Re_2(\mu\text{-}CH)_2(CH_3)_4$, 107201-13-8; $W2(\mu\text{-}CH)_2(OH)_4$, 107201-14-9.

# Preparation, Structure, and Bonding of $Mo_2(OCH_2CMe_3)_6(\mu\text{-}\eta^1,\eta^2\text{-}NCNMe_2)$

Malcolm H. Chisholm,* John C. Huffman, and Nancy S. Marchant

*Department of Chemistry and Molecular Structure Center, Indiana University, Bloomington, Indiana 47405*

*Received October 17, 1986*

Hydrocarbon solutions of $Mo_2(OCH_2\text{-}t\text{-}Bu)_6(M{\equiv}M)$ and $R_2NCN$ (R = Me, Et) react to give a compound of formula $Mo_2(OCH_2\text{-}t\text{-}Bu)_6(\mu\text{-}R_2NCN)$. A single-crystal X-ray diffraction study shows that cyanamide bridges the two molybdenum atoms parallel to the M–M vector. Pertinent bond distances are Mo—Mo = 2.449 (1) Å, C≡N = 1.333 (4) Å, Mo—O (terminal) = 1.91 (average) Å, $Mo_1$–C = 2.014 (4) Å, and $Mo_2$–N = 2.134 (3) Å. $^1H$ NMR studies show the molecule is fluxional at room temperature, involving a turnstile-type motion of three terminal alkoxide ligands. The nature of bonding of the cyanamide ligand to the dimetal center has been investigated by Fenske–Hall calculations on the model system $Mo_2(OH)_6(\mu\text{-}H_2NCN)$. Extensive rehybridization of $H_2NCN$ occurs upon interaction with the dimetal center allowing the cyanamide to act as a donor to both metals. Reduction of the $H_2NCN$ in this compound takes place via back-bonding into the a′ $\pi^*$ orbital of cyanamide. The reduction of the $H_2NCN$ is suggestive of a model for the reaction pathway of RCN with $W_2(O\text{-}t\text{-}Bu)_6$ leading to carbyne and nitride formation.

## Introduction

Prior work has shown $W_2(O\text{-}t\text{-}Bu)_6$ reacts with nitriles to give cleavage of the W≡W and C≡N bond in a metathesis-like manner (eq 1).[1] Similarly, alkynes (though

$$W_2(O\text{-}t\text{-}Bu)_6 + RC{\equiv}N \xrightarrow[\text{alkanes}]{20\ ^\circ C} (t\text{-}BuO)_3W{\equiv}CR + (t\text{-}BuO)_3W{\equiv}N \quad (1)$$

not ethyne) react with $W_2(O\text{-}t\text{-}Bu)_6$ to give alkylidynes $(t\text{-}BuO)_3W{\equiv}CR$.[1,2] Schrock and co-workers have used this metathesis of W≡W and C≡C bonds in the preparation of an extensive class of $(t\text{-}BuO)_3W{\equiv}CR$ compounds which are active toward alkyne metathesis.[3-5] By contrast nitriles and $Mo_2(O\text{-}t\text{-}Bu)_6$ fail to react under similar conditions. Indeed while other N-donor ligands, L, such as pyridine and dimethylamine, reversibly form adducts of formula $Mo_2(OR)_6L_2$ (R = *i*-Pr or $CH_2CMe_3$ = Np),[6,7] nitriles show little affinity to the dimolybdenum center and may be used as solvents. However, dimethylcyanamide, $Me_2NCN$, was shown by Kelly[8] to form 1:1 adducts with $Mo_2(O\text{-}t\text{-}Bu)_6$ and $Mo_2(O\text{-}i\text{-}Pr)_6$ and subsequently was found[9] to undergo the metathesis reaction 1 with $W_2(O\text{-}t\text{-}Bu)_6$. The 1:1 adducts between $Mo_2(OR)_6$ compounds and $Me_2NC{\equiv}N$ became of further interest to us as possible models for intermediates in the metathesis of W≡W and C≡N bonds. In the earlier work of Chisholm and Kelly, crystals suitable for X-ray studies were not obtained for $Mo_2(OR)_6(Me_2NCN)$ compounds. We report here the synthesis and

(1) Schrock, R. R.; Listemann, M. L.; Sturgeoff, L. G. *J. Am. Chem. Soc.* **1982**, *104*, 4291.
(2) Listemann, M. L.; Schrock, R. R. *Organometallics* **1985**, *4*, 74.
(3) Schrock, R. R. *ACS Symp. Ser.* **1983**, *No. 221*, 369.
(4) Wengrovius, J. H.; Sancho, J.; Schrock, R. R. *J. Am. Chem. Soc.* **1981**, *103*, 3932.
(5) Sancho, J.; Schrock, R. R. *J. Mol. Catal.* **1982**, *15*, 75.
(6) Chisholm, M. H.; Cotton, F. A.; Extine, M. W.; Reichert, W. W. *J. Am. Chem. Soc.* **1978**, *100*, 153.
(7) Chisholm, M. H. *Polyhedron* **1983**, 2, 681.
(8) Chisholm, M. H.; Kelly, R. L. *Inorg. Chem.* **1979**, *18*, 2321.
(9) Chisholm, M. H.; Huffman, J. C.; Marchant, N. S. *J. Am. Chem. Soc.* **1983**, *105*, 6162.

0276-7333/87/2306-1073$01.50/0 